

# Integration of synaptic inputs in dendritic trees

## Theoretical Neuroscience

Fabrizio Gabbiani  
Division of Neuroscience  
Baylor College of Medicine  
One Baylor Plaza  
Houston, TX 77030  
e-mail:gabbiani@bcm.tmc.edu

## 1 Introduction

In intact animals, neurons process information by integrating synaptic inputs originating from the presynaptic neurons connected to them. Subsequently they generate action potentials to communicate with their postsynaptic target neurons. Thus, a substantial part of the action takes place in the dendrites of a cell where synaptic inputs are integrated. Our understanding of how synaptic inputs are processed within dendritic trees is much more recent than the understanding of how action potentials are generated and propagate along axons. One reason is that synaptic potentials represent much smaller electrical signals than action potentials and are thus more difficult to record. A second reason is that dendritic structures are small and less accessible to recording electrodes, than for example the giant squid axon. Furthermore, dendrites are very diverse in their shape, synaptic density and distribution of ion channels. In this lecture we want to describe some of the characteristics of synaptic integration in dendritic trees. In particular we will see that:

1. Both excitatory and inhibitory subthreshold conductance changes due to synaptic transmission interact non-linearly.
2. The summation of postsynaptic potentials depends both on the location of synaptic inputs in a dendritic tree and on their temporal pattern of activation.
3. Activation of synaptic inputs can be expected to have a large effect on the electrotonic structure of a cell, which in turn will contribute to changing the integration of synaptic inputs in a dynamic way.
4. Active membrane conductances located in the dendrites significantly affect the integration of synaptic inputs.

These aspects of synaptic integration are by now fairly well established. However, it is important to stress that the way in which dendritic integration properties combine to determine how information is processed by neurons is still poorly understood and constitutes an active area of research.

One important ingredient of synaptic integration that we have not yet discussed is inhibition. We therefore start by describing inhibition originating from  $GABA_A$  synaptic conductances and then analyse some simple models for the interaction of synaptic inputs in dendritic trees.

## 2 Synaptic inhibition

The predominant chemical inhibitory synaptic transmitter substance is GABA ( $\gamma$ -aminobutyric acid), although other substances like glycine in the vertebrate spinal cord, histamine in arthropod photoreceptors and acetylcholine in molluscan neurons also have inhibitory effects. GABA binds onto several distinct receptor channels that mediate different types of postsynaptic signals. Fast inhibitory synaptic transmission is mediated by  $GABA_A$

receptors while slower, second messenger mediated inhibitory synaptic transmission occurs through  $GABA_B$  and  $GABA_C$  receptors. We will here concentrate on fast  $GABA_A$  transmission. Upon binding onto  $GABA_A$  receptors,  $GABA$  causes the opening of  $Cl^-$ -selective ion channels allowing an inward flow of  $Cl^-$  (and thus an outward flow of positive current). An important property of these channels is that the reversal potential for chloride ions is close to the resting potential of the cell. Indeed, as we have seen in previous lectures,  $Cl^-$  ions are thought to be in large part responsible for the resting conductance of neurons. Thus the effect of  $GABA$  is more easily detected when a neuron is depolarized above rest, because the driving force of the chloride reversal potential then tends to bring the membrane potential back towards its resting value. When the membrane potential is close to rest, as is the case most of the time during normal conditions, the main effect of  $GABA$  is to increase the conductance of the neuronal membrane. Excitatory synaptic transmission increases the conductance of the membrane as well, but because the reversal potential is far from rest (typically  $\sim 80$  mV positive with respect to rest) the most conspicuous effect of excitation is to shift the membrane potential away from its resting value. For this reason fast inhibitory synaptic transmission is often said to be *silent* or of the *shunting* type. We will see in the next sections that this asymmetry between excitation and inhibition has several consequences on the integration of synaptic inputs by neurons.

The dynamics of synaptic transmission (both excitatory and inhibitory) can be obtained from detailed biophysical models of the opening and closing of the corresponding ion channels in response to neurotransmitter substances. As we have seen in a previous lecture, this is particularly important in the case of NMDA receptor-mediated synaptic transmission since the conductance of the corresponding channel is voltage dependent. In contrast, most other ionic synaptic channels behave to a good approximation as perfect (ohmic) resistors and we can therefore restrict ourselves to a phenomenological description of the time-course of conductance change corresponding to the activation of a few hundred such channels simultaneously in response to release of a synaptic vesicle. A choice that works quite well in practice is the  $\alpha$  function model:

$$g_{syn}(t) = C \cdot t e^{-t/t_{peak}}.$$

This function increases from a value of 0 at  $t = 0$  and peaks at  $t_{peak}$  (as may be seen by setting the derivative  $g'_{syn}(t) = 0$ ) before decaying towards rest. The constant  $C$  is chosen such that the peak conductance  $g_{peak}$  is reached at  $t_{peak}$ , i.e.,  $C = g_{peak} \cdot e/t_{peak}$ .

### 3 Steady-state patch model of synaptic integration

A simple way to investigate synaptic integration is to use the patch membrane model of the previous lectures (Fig. 1). In addition to the membrane capacitance ( $c_m$ ) and resting conductance ( $g_r$ ; reversal potential:  $v_r$ ), we introduce two synaptic conductances  $g_e$  and  $g_i$  with reversal potentials  $v_e$  and  $v_i$ , respectively. These conductances will be interpreted as excitatory and inhibitory synaptic conductances, respectively. Because our calculations are general, we can also interpret  $g_i$  as a second excitatory input by setting its value equal

to  $g_e$ . The membrane voltage  $v_m$  obeys the familiar differential equation,

$$c_m \frac{dv_m}{dt} + g_r(v_m - v_r) + g_e(v_m - v_e) + g_i(v_m - v_i) = i_m,$$

where  $i_m$  is an external current (for example applied through an electrode or flowing from a different dendritic compartment). We make an important simplification by taking  $g_e = \text{constant}$ ,  $g_i = \text{constant}$  and  $i_m = \text{constant}$ . The assumptions of time-independent synaptic activation is of course unrealistic since, as we have seen above, usually an  $\alpha$  function is needed to describe the kinetics of synaptic activation. The advantage of this approximation is that it will allow us to solve exactly for the membrane voltage and thus yield useful insight on the effect of synaptic inputs on membrane voltage dynamics. We define the membrane time constant,  $\tau_m = c_m/g_r$ , the ratio of excitatory to resting membrane conductance,  $c_e = g_e/g_r$  and the ratio of inhibitory to resting membrane conductance,  $c_i = g_i/g_r$ . If we set

$$\tau' = \frac{\tau_m}{1 + c_e + c_i}, \quad v_{ss} = \frac{v_r + c_e v_e + c_i v_i + i_m/g_r}{1 + c_e + c_i},$$

we can rewrite the above equation as

$$\tau' \frac{dv_m}{dt} = -v_m + v_{ss},$$

and the solution is

$$v_m(t) = v_{ss} - (v_{ss} - v_m(0))e^{-t/\tau'}. \quad (1)$$

Thus, the membrane potential relaxes exponentially to its steady state value  $v_{ss}$ . We can now make several interesting observations from this simple model.

## 4 Local summation of excitatory and inhibitory inputs

**Single excitatory input.** We first look at the simplest case of a single excitatory input on the patch: assume  $i_m = 0$  and  $c_i = 0$ . The steady-state potential is given by

$$v_{ss} = \frac{v_r + c_e v_e}{1 + c_e},$$

and rearranging,

$$v_{ss} = v_r + \frac{c_e}{1 + c_e}(v_e - v_r). \quad (2)$$

This last equation tells us that the steady state membrane potential depolarization depends in a sigmoidal way on the fraction of activated excitatory conductances,  $c_e$  and *saturates* at  $v_e - v_r$ . This makes intuitive sense, since when  $v_e - v_r$  is reached the driving force of the excitatory input cannot drive further current into the cell.

**Two excitatory inputs.** What happens if two identical excitatory synaptic conductances are activated in the same compartment? In our previous patch model this corresponds to setting  $v_i = v_e$ ,  $c_i = c_e$ ,  $i_m = 0$ . We then have

$$v_{ss} = \frac{v_r + 2c_e v_e}{1 + 2c_e}.$$

We can again rearrange the equation to see how the activation of the synaptic conductances shifts the membrane potential from rest,

$$v_{ss} = v_r + \frac{2c_e}{1 + 2c_e}(v_e - v_r).$$

How does this compare to the depolarization predicted by the linear sum of two inputs? According to eq. 2 we expect

$$v_{ss} = v_r + \frac{2c_e}{1 + c_e}(v_e - v_r).$$

Thus, we see that summation of 2 excitatory inputs is highly non-linear (Fig. 2).

**One excitatory and one inhibitory input.** We now investigate what happens when the second input corresponds to shunting inhibition:  $v_i = v_r$  and  $i_m = 0$ . We obtain

$$\begin{aligned} v_{ss} &= \frac{v_r + c_e v_e + c_i v_r}{1 + c_e + c_i} \\ &= v_r + \left( \frac{v_r + c_e v_e + c_i v_r}{1 + c_e + c_i} - v_r \right), \end{aligned}$$

and rearranging,

$$v_{ss} = v_r + \frac{c_e}{1 + c_e + c_i}(v_e - v_r).$$

This is essentially the same result as obtained for two excitatory inputs above. When  $c_i \gg 1 + c_e$  (or equivalently, when  $g_i \gg g_r + g_e$  we can simplify to obtain

$$v_{ss} \cong v_r + \frac{c_e}{c_i}(v_e - v_r).$$

In other words, shunting inhibition has a *divisive* effect on membrane potential (Fig. 2).

## 5 Impact of electrotonic parameters on synaptic activation

**Membrane time constant.** Another important aspect of synaptic activation is its effect on the passive properties of a membrane patch or a dendritic cable. Of course, activation of additional conductances reduces the input resistance of the patch or, equivalently, increases its conductance. One immediate consequence is seen in eq. 1 for the time-dependent convergence towards steady-state. As usual, the membrane potential relaxes

exponentially towards steady-state but the time constant of relaxation is not the membrane time constant  $\tau$  any more. It is rather the membrane time constant scaled by the relative value of conductances opened by synaptic activation. If we define  $c_{tot} = c_e + c_i$  we have  $\tau' = \tau / (1 + c_{tot})$ . Thus the opening of additional channels causes the membrane potential response of the cell to be faster than at rest. To get a better feeling for the magnitude of the effect, we study a specific example. Assume that the specific membrane conductivity is  $R_m = 50,000 \Omega \cdot cm^2$ , a plausible value for a dendritic membrane patch. The corresponding conductance per micrometer of square area is  $G_m = 2 \cdot 10^{-4} nS/\mu m^2$  and if we consider a spherical patch of membrane of radius  $r = 15 \mu m$  we obtain a total area ( $4\pi r^2$ ) of  $\cong 2827 \mu m^2$  and therefore an input conductance of  $\cong 0.57 nS$ . Since a typical synaptic activation results in a peak conductance change of approximately  $0.5 nS$  we see that a single synapse would nearly decrease by a factor two the membrane time constant in such a case.

**Dendritic cable constant.** A characteristic property of dendritic cables is their *space constant*, defined as

$$\lambda = \sqrt{\frac{R_m d}{R_i 4}} = \sqrt{\frac{G_i d}{G_m 4}},$$

where  $G_m = R_m^{-1}$  is the specific membrane conductance (conductance per unit area; the typical units of the specific membrane resistance,  $R_m$ , are  $\Omega \cdot cm^2$ ) of the cable membrane. The constant  $G_i = R_i^{-1}$  is the specific intracellular conductivity (in units of conductance per unit length; the typical units of the intracellular resistivity,  $R_i$ , are  $\Omega \cdot cm$ ). Note that  $R_i$  is often called  $R_2$  in the literature, and we have used this alternative notation in previous lectures. The number  $d$  is the diameter of the cable. The space constant characterizes the distance over which the membrane potential is attenuated along the cable. For example, during injection of a constant current in the middle of an infinite cable, the membrane potential decays exponentially along the cable and reaches 37% ( $e^{-1}$ ) of its value at a distance from the injection point equal to the space constant. Therefore a doubling of the specific membrane conductance will decrease the space constant by a factor  $\sqrt{2}$ . This means that the electrotonic length of a cable (its real length measured in units of the space constant) will increase by the same factor. Thus activation of synaptic conductances will also modify the net effect of currents at a distance and increase the relative electrical separation of points along a cable.

To justify these statements we consider again the cable equation,

$$C_m \frac{\partial V}{\partial t} + g_L V = G_i \frac{\partial^2 V}{\partial x^2}.$$

We first multiply both sides by  $R_m$ . By using the definition of the membrane time constant,  $\tau_m = R_m C_m$  and the above definition of the space constant we can rewrite:

$$\tau_m \frac{\partial V}{\partial t} + V = \lambda^2 \frac{\partial^2 V}{\partial x^2}.$$

It is now easy to see that if  $V(x, t)$  is a solution of the cable equation above, then the scaled version  $\tilde{V}(\tilde{x}, \tilde{t}) = V(x/\lambda, t/\tau)$  is a solution of

$$\frac{\partial \tilde{V}}{\partial \tilde{t}} + \tilde{V} = \frac{\partial^2 \tilde{V}}{\partial \tilde{x}^2} \quad \text{where} \quad \tilde{x} = x/\lambda, \quad \tilde{t} = t/\tau.$$

Consider two dendritic cables extending from  $[0; l]$  and  $[0; 2l]$  that have cable constants  $\lambda$  and  $2\lambda$ , respectively. If current is injected at one end of both cables, then a point  $x = \alpha l$ , with  $\alpha \in [0; 1]$  on the first cable will experience the same depolarization as the point  $x' = \alpha \cdot 2l$  on the second cable. Thus,  $\lambda$  is a measure of the electrical length of the cable. To see this in a specific example, let us consider a finite cable of extent  $[0; l]$  that receives a constant current pulse  $I_0$  at  $x = 0$ . We concentrate on the steady-state solution of the cable equation, i.e., the membrane potential,  $V(x, t \rightarrow \infty)$ , once transients have settled down. This steady-state membrane potential,  $V_{ss}(x)$  satisfies a differential equation that is obtained from the cable equation by setting the time-dependent derivative equal to zero:

$$\lambda^2 \frac{d^2 V_{ss}}{dx^2} = V_{ss} \quad (\text{steady-state cable equation}),$$

with boundary conditions,

$$\left. \frac{dV_{ss}}{dx} \right|_{x=0} = -\gamma, \quad \left. \frac{dV}{dx} \right|_{x=l} = 0,$$

where  $\gamma = I_0 R_2 / A_c$  is the injected current scaled by the intracellular resistivity  $R_2 = R_i$  and the cross-sectional area of the cable. The solution of this equation is obtained from the *Ansatz*,  $V_{ss}(x) = c_1 e^{x/\lambda} + c_2 e^{-x/\lambda}$ ,

$$V_{ss}(x) = V_{ss}(0) \frac{\cosh(\frac{l-x}{\lambda})}{\cosh(l/\lambda)}. \quad (3)$$

We see directly from this equation that if  $\lambda \rightarrow 2\lambda$  and  $l \rightarrow 2l$  then the same steady state membrane potential is obtained at  $x_0$  in the first cable and at  $2x_0$  in the second cable. In the limit of an infinite cable  $l \rightarrow \infty$  we obtain

$$V_{ss}(x) = V_{ss}(0) e^{-x/\lambda}. \quad (4)$$

Thus, in this limit the cable constant uniquely characterizes the decay of the membrane potential as a function of distance from the current injection point. The approximation  $l \rightarrow \infty$  is only valid if the length of a dendritic cable is much larger than the cable constant, which is usually not the case. Thus  $\lambda$  gives only an approximate but intuitively simple characterization of the electrical length of the cable.

All the effect described above (decrease in input resistance, decrease in time constant and increase in electrotonic length) are expected to play a role in synaptic integration. In vivo, neurons receive constant background synaptic activity from other neurons to which they are connected. Spontaneous activity rates are on the order of  $\sim 5$  spk/s.

If each neuron receives 5,000 synaptic inputs (typical cortical neurons will receive from 5,000 to 20,000 such inputs), this corresponds to 25,000 activated synapses per second. Although each such activation affects minimally the electrotonic properties of a neuron, the combined effect can be expected to be large. Simulations show that cortical pyramidal cells can be expected to see their membrane time constant decrease by a factor five due to spontaneous activity (Fig. 4). Similarly their electrotonic length will increase by a factor  $\sim 2$ . Similar, but considerably larger changes are expected during sensory processing, when many more inputs are activated simultaneously. Thus one should not think of a neuron as having static electrical parameters. Its electrical properties change dynamically as a function of time due to spontaneous or evoked activity.

## 6 Proximal vs. distal inhibition

The relative location of synaptic inputs can also be expected to play a role in their integration. We illustrate this by considering a model consisting of two compartments in series and investigating the interaction between two inputs, one excitatory and the other inhibitory, depending on their location (Fig. 1). The first compartment should be thought of being distal to the spike initiation zone of the neuron. It could represent the dendritic tree of the neuron for example. The second compartment should be thought of being more proximal to the spike initiation zone and could for example represent the soma of the neuron. We investigate the effect of inhibition, either placed proximally or distally, on the activation of excitatory distal input. Anatomical evidence suggests that inhibition is often placed in these two different positions with respect to excitatory inputs.

**Proximal inhibition.** The circuit diagram illustrated in Fig. 1. The circuit leads to the following two equations, obtained by applying Kirchoff's law:

$$\begin{aligned} c_p \frac{dv_p}{dt} + g_p(v_p - v_r) + g_i(v_p - v_i) + g_{dp}(v_p - v_d) &= 0, \\ c_d \frac{dv_d}{dt} + g_d(v_d - v_r) + g_e(v_d - v_e) + g_{dp}(v_d - v_p) &= 0, \end{aligned}$$

where  $g_{p/d}$  and  $c_{p/d}$  are the conductance and capacitance of the proximal (distal) compartments,  $g_{e/i}$  are the conductance of the excitatory (inhibitory) synapses and  $g_{dp}$  is the axial conductance between the two compartments. We now assume that  $dv_p/dt = dv_d/dt = 0$  and that the activated conductances are time independent. Of course these steady-state assumptions are not realistic, but they will allow us to solve for the membrane potential in the proximal compartment exactly and therefore allow us to gain insight in the effect of proximal inhibition on distal excitation. Under these assumptions, the equation system above reduces to an algebraic equation for  $v_p$  and  $v_d$ ,

$$\begin{aligned} g_p(v_p - v_r) + g_i(v_p - v_i) + g_{dp}(v_p - v_d) &= 0, \\ g_d(v_d - v_r) + g_e(v_d - v_e) + g_{dp}(v_d - v_p) &= 0. \end{aligned} \tag{5}$$

We further assume that  $v_i = v_r$ , i.e., inhibition is of the shunting type and redefine the potentials with respect to rest,

$$\tilde{v}_p = v_p - v_r, \quad \tilde{v}_d = v_d - v_r, \quad \tilde{v}_e = v_e - v_r.$$

The algebraic system of equations 5 may be rewritten as

$$\begin{aligned} (g_p + g_i + g_{dp})\tilde{v}_p - g_{dp}\tilde{v}_d &= 0, \\ -g_{dp}\tilde{v}_p + (g_p + g_e + g_{dp})\tilde{v}_d &= g_e\tilde{v}_e. \end{aligned}$$

Setting  $a = (g_p + g_i + g_{dp})$ ,  $b = c = -g_{dp}$ ,  $d = (g_p + g_e + g_{dp})$  we have

$$\mathbf{A} \begin{pmatrix} \tilde{v}_p \\ \tilde{v}_d \end{pmatrix} = \begin{pmatrix} 0 \\ g_e\tilde{v}_e \end{pmatrix}, \quad \begin{pmatrix} \tilde{v}_p \\ \tilde{v}_d \end{pmatrix} = \mathbf{A}^{-1} \begin{pmatrix} 0 \\ g_e\tilde{v}_e \end{pmatrix},$$

with

$$\mathbf{A} = \begin{pmatrix} a & b \\ c & d \end{pmatrix}, \quad \mathbf{A}^{-1} = \frac{1}{ad - b^2} \begin{pmatrix} d & -c \\ -b & a \end{pmatrix}.$$

A straightforward calculation yields  $ad - b^2 = \alpha + \beta g_e + \gamma g_i + g_e g_i$  with  $\alpha = g_d g_p + g_d g_{dp} + g_p g_{dp}$ ,  $\beta = g_p + g_{dp}$ ,  $\gamma = g_d + g_{dp}$  and we can now solve for  $\tilde{v}_p$ :

$$\tilde{v}_p = \frac{g_e g_{dp} \tilde{v}_e}{\alpha + \beta g_e + \gamma g_i + g_e g_i}.$$

The best way to understand the significance of this equation is to plot a specific case (see Appendix A.1). We can nevertheless get an understanding of its significance by looking at the behavior of  $\tilde{v}_p$  when the excitatory conductance is large:

$$\lim_{g_e \rightarrow \infty} \tilde{v}_p = \frac{g_{dp} \tilde{v}_e}{\beta + g_i}. \quad (6)$$

This equation tells us that, no matter how large the excitatory input is, the inhibitory input can effectively act as a *veto* to excitation: it is always possible to increase the inhibitory conductance ( $g_i$ ) and overcome the effect of excitation.

**Distal inhibition.** When inhibition is located in the same distal compartment as excitation, Kirchoff's law yields the following current conservation equations:

$$\begin{aligned} c_p \frac{dv_p}{dt} + g_p(v_p - v_r) + g_{dp}(v_p - v_d) &= 0, \\ c_d \frac{dv_d}{dt} + g_d(v_d - v_r)g_e(v_d - v_e) + g_i(v_d - v_i) + g_{dp}(v_d - v_p) &= 0. \end{aligned}$$

We can now rearrange using the same assumptions as in the proximal inhibition case,

$$\begin{aligned} (g_p + g_{dp})\tilde{v}_p - g_{dp}\tilde{v}_d &= 0, \\ -g_{dp}\tilde{v}_p + (g_d + g_e - g_i + g_{dp})\tilde{v}_d &= g_e\tilde{v}_e. \end{aligned}$$

Defining  $a = (g_p + g_{dp})$ ,  $b = c = -g_{dp}$ ,  $d = (g_d + g_e + g_i + g_{dp})$ , we obtain  $ad - b^2 = \alpha + \beta g_e + \beta g_i$  and therefore,

$$\tilde{v}_p = \frac{g_{dp} g_e \tilde{v}_e}{\alpha + \beta g_e + \beta g_i}. \quad (7)$$

Once again, this equation is best understood by plotting it (Appendix A.1. Taking the same limit as in the proximal inhibition case, we obtain

$$\lim_{g_e \rightarrow \infty} \tilde{v}_p = \frac{g_{dp} \tilde{v}_e}{g_p + g_{dp}}.$$

The important difference with eq. (6) is that distal inhibition cannot veto excitation. In other words, an increase of excitation can always overcome distal inhibition since the limiting value is independent of  $g_i$ .

## 7 Spatio-temporal activation patterns of synaptic inputs

By now we have seen that synaptic inputs interact non-linearly and that these interactions depend on relative spatial location. We have also seen that background synaptic inputs can significantly affect the electrotonic properties of a neuron. What about temporal effects? All our calculations have concentrated on steady-state conductance changes because they are amenable to exact solution, but realistic inputs have both spatial and temporal activation profiles.

The first important temporal effect that we describe has to do with the membrane potential spread along a dendritic cable following activation of an excitatory synaptic input. As one moves further away from the site of EPSP activation, the peak membrane potential depolarization decreases, due to loss of current through membrane conductances along the cable. The second effect is a spread of the membrane potential depolarization in time. Thus, the farther away one is from the site of activation, the more spread out in time the depolarization is. This is due to low-pass filtering caused by the passive cable.

Simulations also show that the spatiotemporal pattern of activation of excitatory synaptic inputs along a dendritic cable can have a significant effect on the depolarization observed at the soma of a neuron. This is illustrated in Fig. 3. In this example, the same excitatory inputs are activated along a dendritic cable, but their sequence of activation differs. The inputs are activated from the dendritic periphery towards the trunk in the first case and using the opposite sequence in the second case. As one can see from the figure, this results in distinctly different temporal shapes of the postsynaptic potential at the soma, and a reduced peak depolarization in the trunk-to-distal case. Such spatiotemporal activation patterns along a dendritic cable are thought to contribute to directional selective responses observed in certain retinal ganglion cells.

## 8 Effect of active conductances on synaptic integration

In the past decades, it has become increasingly clear that the dendrites of neurons are not well approximated as passive cables. There are a number of voltage dependent conductances that are present in dendrites and that could potentially influence the integration of synaptic inputs. One early conductance that was reported to be localized in the dendritic tree of cerebellar Purkinje cells is a transient potassium current called the A-current ( $I_A$ ). Recently it has become clear that many cortical neurons possess an H-current ( $I_H$ ) in their dendritic trees and that the density of channels increases with the distance from the soma. This current is very unusual because it is a mixed  $Na^+K^+$  conductance with a reversal potential above resting membrane potential (typically between -20 and -40 mV with respect to the extracellular potential). Furthermore the conductance opens fully when the membrane potential is *hyperpolarized* and will therefore tend to bring back the membrane potential towards rest in such cases. The H current is estimated to be active at about 7-8% of its peak conductance at rest. One important consequence of the higher density of  $I_H$  in the dendrites is that the membrane conductance is increased, leading to a shorter time window for summation of excitatory inputs. Drugs that block  $I_H$  show increased summation of excitatory inputs, particularly for dendritic EPSPs.

## A Appendix

### A.1 Plot of $\tilde{v}_p$ as a function of the excitatory conductance

We plot  $\tilde{v}_p$  using values proposed by Vu and Krasne in an article investigating the effect of proximal and distal inhibition on the generation of escape responses in crayfish. We assume  $\tilde{v}_e = 100$  mV,  $g_p = g_d$  and  $R_p/R_p + R_{dp} = 0.1$  or equivalently  $g_{dp} = (1/9)g_p$ . From these assumptions we can first compute  $\alpha = \alpha_0 g_d^2$ , with  $\alpha_0 = 1 + 2/9$ ,  $\beta = \beta_0 g_d$ , with  $\beta_0 = 1 + 1/9$  and  $\beta = \gamma$ . In the proximal inhibition case, we obtain

$$\tilde{v}_p = \frac{1}{9} \frac{g_e}{g_d} \tilde{v}_e \cdot \frac{1}{\alpha_0 + \beta_0 \left( \frac{g_e}{g_d} + \frac{g_i}{g_d} \right) + \frac{g_e g_i}{g_d g_d}}.$$

Setting  $x = g_e/g_d$ ,  $y = g_i/g_d$  we obtain

$$\tilde{v}_p = \frac{\tilde{v}_e}{9} \frac{x}{\alpha_0 + \beta_0(x + y) + xy}.$$

In the distal inhibition case we have

$$\tilde{v}_p = \frac{1}{9} \frac{g_e}{g_d} \tilde{v}_e \frac{1}{\alpha_0 + \beta_0 \frac{g_e}{g_d} + \beta_0 \frac{g_i}{g_d}},$$

and using the same conventions as above,

$$\tilde{v}_p = \frac{\tilde{v}_e}{9} \frac{x}{\alpha_0 + \beta_0(x + y)}.$$

## Figure Legends

**Figure 1.** Schematics of a single patch and of 2-compartment electrotonic models with proximal and distal inhibitory synapses, respectively.

**Figure 2.** Top: Summation of two excitatory inputs at steady-state in a local patch of membrane. Bottom: Divisive effect of inhibition on excitatory postsynaptic responses.

**Figure 3.** Effect of spatiotemporal sequences of excitatory inputs on a soma dendrite model (10 compartments, compartment 1 is the soma). An excitatory conductance pulse is activated simultaneously at two locations ( $\epsilon$ , top insets) for the duration indicated at the bottom on the abscissa. Membrane depolarization is reported normalized with respect to the rest ( $E_r$ ) and excitatory reversal potentials ( $E_\epsilon$ ). The dotted curve is the response to total activation of the same conductance distributed over compartments 2 through 9 over the same time period ( $t/\tau$  from 0 to 1). Adapted from Rall, 1964.

**Figure 4.** Effect of mean background activity ( $\langle f_b \rangle$ ) on input resistance, membrane time constant, electrotonic length and resting potential in a single cable, a passive and an active pyramidal cell model. Adapted from Koch, 1999.

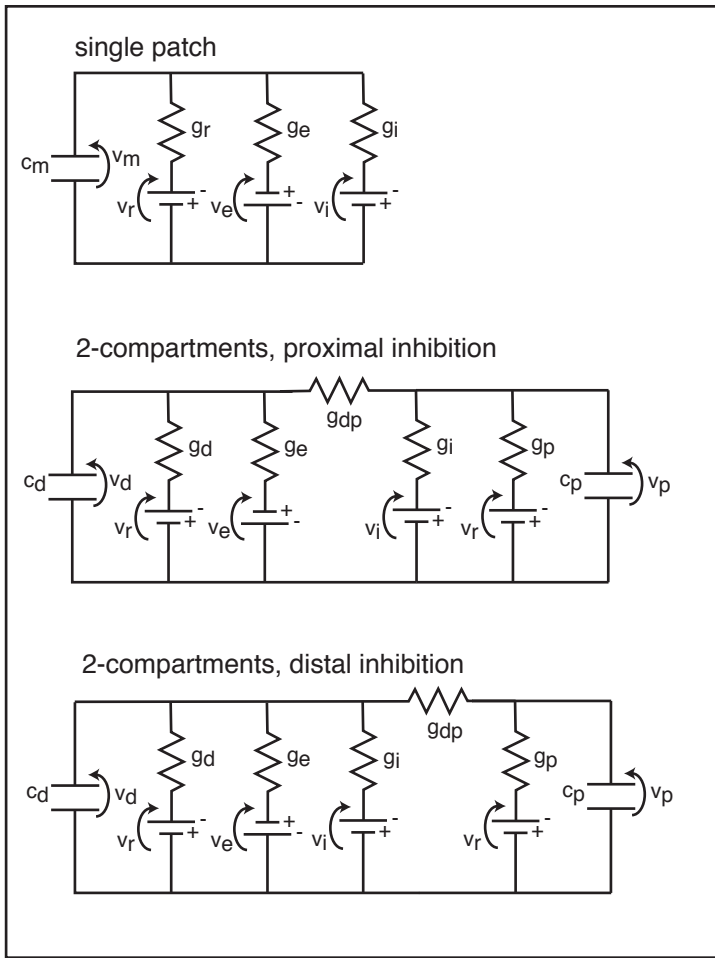


Figure 1

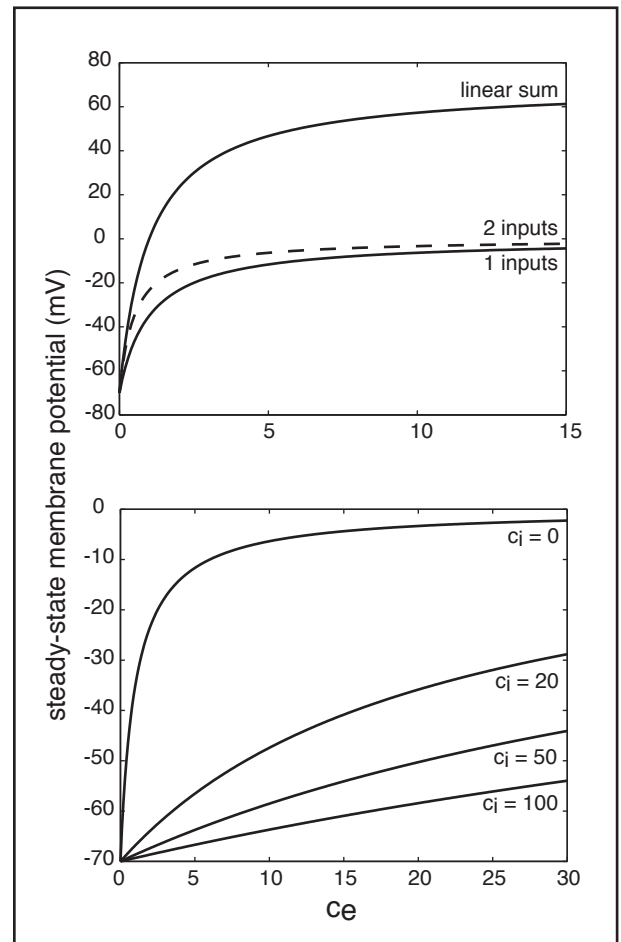


Figure 2

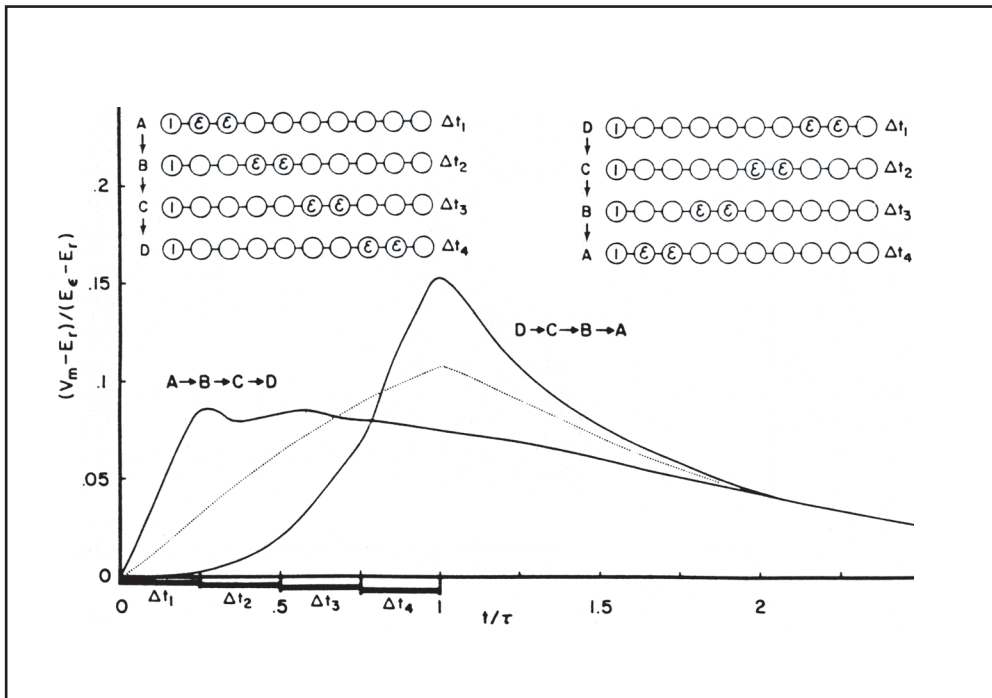


Figure 3

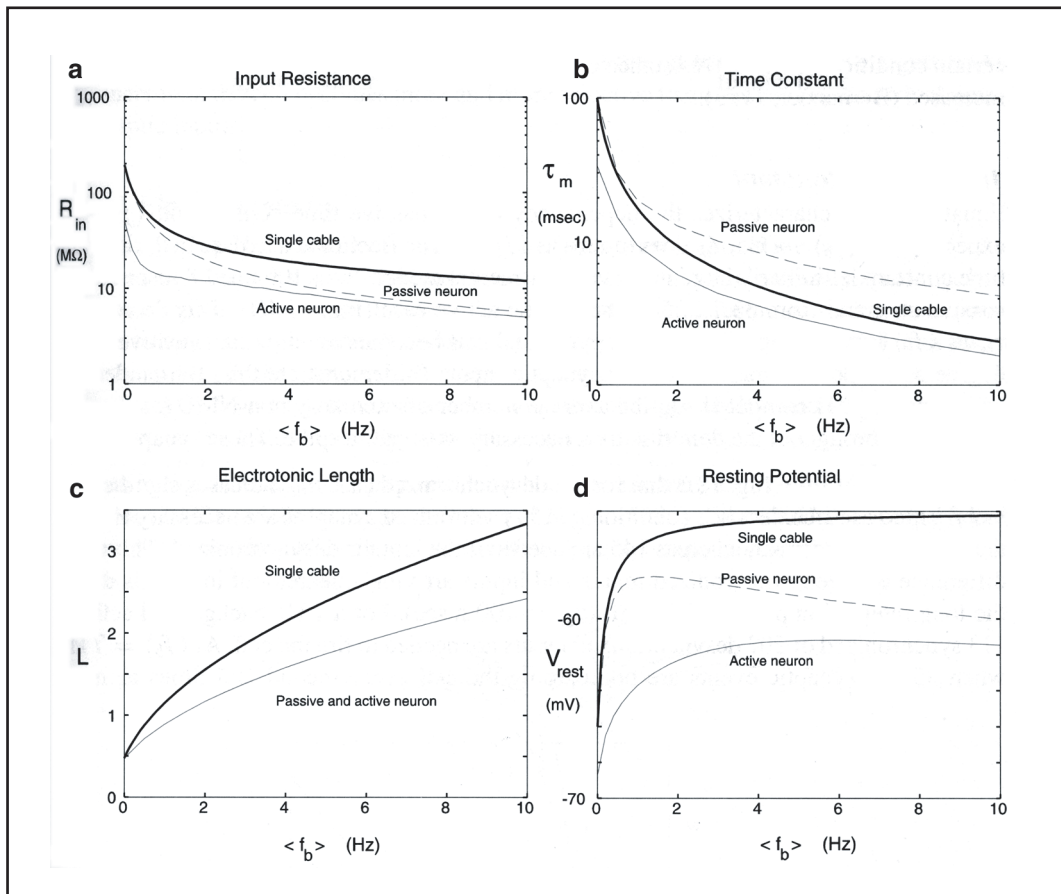


Figure 4